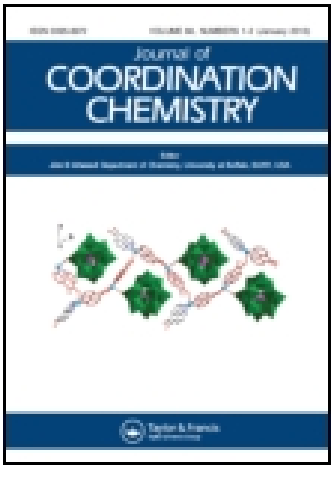

Journal of Coordination Chemistry
Publication details, including instructions for authors and subscription information:
http://www.tandfonline.com/loi/gcoo20

New silver(I) pyridinecarboxylate complexes: synthesis, characterization, and antimicrobial therapeutic potential

Z. Vargová[a], M. Almáši[a], D. Hudecová[b], D. Titková[a], I. Rostášová[a], V. Zeleňák[a] & K. Györyová[a]

[a] Faculty of Science, Department of Inorganic Chemistry, P. J. Šafárik University, Košice, Slovak Republic

[b] Department of Biochemistry and Microbiology, Slovak University of Technology, Bratislava, Slovak Republic

Accepted author version posted online: 20 Mar 2014.Published online: 17 Apr 2014.

To cite this article: Z. Vargová, M. Almáši, D. Hudecová, D. Titková, I. Rostášová, V. Zeleňák & K. Györyová (2014) New silver(I) pyridinecarboxylate complexes: synthesis, characterization, and antimicrobial therapeutic potential, Journal of Coordination Chemistry, 67:6, 1002-1021, DOI: 10.1080/00958972.2014.906588

To link to this article: http://dx.doi.org/10.1080/00958972.2014.906588

Journal of Coordination Chemistry, 2014
Vol. 67, No. 6, 1002–1021, http://dx.doi.org/10.1080/00958972.2014.906588

New silver(I) pyridinecarboxylate complexes: synthesis, characterization, and antimicrobial therapeutic potential

Z. VARGOVÁ*†, M. ALMÁŠI†, D. HUDECOVÁ‡, D. TITKOVÁ†, I. ROSTÁŠOVÁ†, V. ZELEŇÁK† and K. GYÖRYOVÁ†

†Faculty of Science, Department of Inorganic Chemistry, P. J. Šafárik University, Košice, Slovak Republic
‡Department of Biochemistry and Microbiology, Slovak University of Technology, Bratislava, Slovak Republic

(*Received 13 November 2013; accepted 26 February 2014*)

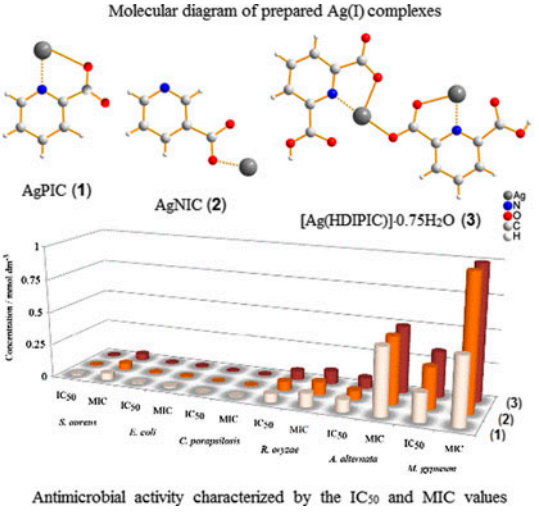

Antimicrobial activity characterized by the IC_{50} and MIC values

Silver(I) pyridinecarboxylates (AgPIC (**1**), AgNIC (**2**), [Ag(HDIPIC)]·0.75H_2O (**3**), PIC = picolinate, NIC = nicotinate, HDIPIC = dipicolinate) were prepared by solvothermal syntheses and their characterization were completed by elemental, spectral, and thermal analyses. To assign the pyridinecarboxylate coordination mode in the complexes, detailed mid-infrared spectral data and $\Delta(\nu_{as} - \nu_s)$ comparisons were accomplished. In addition, silver(I) pyridinecarboxylate antimicrobial activities and stability by ^{1}H NMR spectra were determined. Moreover, the spectral, thermal, and antimicrobial properties of silver(I) and previously prepared zinc(II) pyridinecarboxylates were compared and discussed.

*Corresponding author. Email: zuzana.vargova@upjs.sk

Keywords: Silver(I) complexes; Pyridinecarboxylic acids; Mid-IR spectra; ^{1}H NMR spectra; Thermal analysis; Antimicrobial activity

1. Introduction

The vast majority of antimicrobial drugs used to date are purely organic (synthetic or natural) compounds. However, resistance of pathogens towards currently used antibiotics is evident [1]. Bioinorganic chemistry is an emerging field in medicinal chemistry, which offers the biological (and therapeutic) potential of inorganic complexes [2–4]. Metal compounds (Zn(II), Al(III), Ag(I), etc.) play significant roles during microbial infection treatment [5]. As a result of their different coordination geometries, chemical properties, and reactivities, metal complexes offer a wide spectrum of functional groups unexplored in modern drug design and development [6].

The carboxylic (mainly aromatic – benzoic or salicylic) acids as O-donors are often used as antimicrobial agents during food preservation (sodium benzoate with E number E211) [7] or as anti-inflammatory drugs in cosmetics [8].

Pyridinecarboxylic acids as N-, O-donors are significant biomolecules. Picolinic acid [pyridine-2-carboxylic acid or HPIC, scheme 1(a)] as a catabolite of the amino acid tryptophan is a chelating agent of chromium, zinc, manganese, copper, iron, and molybdenum in the human body [9]. It is present in dietary additives as a carrier of divalent zinc and chromium cations [10]. Nicotinic acid (niacin) [pyridine-3-carboxylic acid or HNIC, scheme 1(b)] is a water-soluble essential vitamin for redox [11, 12] and non-redox [13, 14] reactions. Dipicolinic acid [pyridine-2,6-dicarboxylic acid or H_2DIPIC, scheme 1(c)] composes 5 to 15% of the dry weight of bacterial spores [15]. Therefore, it can be used as an indicator of spores in hospitals, childcare centers, dentists' offices, nursing homes, and spacecrafts [16].

Their prevalent coordination modes are N-, O-chelate for picolinate [scheme 2(a)] and dipicolinate [scheme 2(c)] and N-, O-bridging for nicotinate [scheme 2(b)]. Commonly preferred coordination modes registered in CCDC database are shown in scheme 2.

Ag(I) pyridinecarboxylates, [Ag(HPIC)(PIC)]·H_2O [17], *catena*-H[Ag(NIC)$_2$] [18], *catena*-[Ag(NIC)] [19], and Ag(II) pyridinecarboxylate [Ag(DIPIC)$_2$]·H_2O [20] were previously prepared and their composition and silver(I) coordination mode confirmed by crystal structure determination (registered in CCDC). Spectroscopic studies of Ag(picolinate) were noted and compared with Fe(III), Zn(II), Cu(II), and Ni(II) picolinates [21]. Moreover, Abarca *et al.* [22] used $\nu(COO^-)$ separations for pyridinecarboxylate bond determination. The Ag–COO^- bond was determined as ionic, since the wavenumber was 1610 cm^{-1} or lower. Higher COO^- group wavenumbers would indicate an increase in the covalent character of the Ag–COO^- bond. In addition, symmetrical vibrations at 1450–1350 cm^{-1} were used for correlation between bond character and $\Delta(\nu_{as} - \nu_s)$ variations. When the differences in wavenumbers increase, bonding among the metal and the carboxylate groups becomes more covalent. Thus, their AgPIC (composition stoichiometry: Ag(PIC)$_2$·H_2O) complex ($\Delta = 229$ cm^{-1}) provides mostly covalent bonding and AgNIC (composition stoichiometry: Ag(NIC)$_2$) complex ($\Delta = 208$ cm^{-1}) an ionic bond. Moreover, these results are in accord with X-ray characterizations of *catena*-H[Ag(NIC)$_2$] (Ag–O distance is 2.80–2.83 Å), which is unusually long in comparison to [Ag(HPIC)(PIC)]·H_2O (2.524 Å) [22].

Silver and its compounds have long been used as antimicrobial agents. Silver sulfadiazine insoluble polymeric complex (sulfadiazine = N,O-donor) is a widely used broad-spectrum antibiotic [23, 24] which slowly releases Ag(I) in the wound [5]. The influence of silver coordination mode and donor type to silver antimicrobial agents activity was analyzed in literature [25].

Silver(I) pyridinecarboxylates' {AgNIC (as $Ag(NIC)_2$), AgPIC (as $Ag(PIC)_2 \cdot H_2O$), AgISONIC, AgQUINOL, AgLUTIDIN, and AgISOCINCHOM (ISONIC = isonicotinate, QUINOL = quinolinate, LUTIDIN = lutidinate, ISOCINCHOM = isocinchomeronate)} antibacterial behavior (selected bacteria *Escherichia coli* and *Streptococcus agalactiae*) was previously analyzed [22]. Their antifungal activity was not observed until now.

Zn(II) pyridinecarboxylates were previouly prepared and their crystal structures are recorded in CCDC with pyridinecarboxylate coordination modes *a*, *b*, *c* (scheme 2). Moreover, $[Zn(NIC)_2(H_2O)_4]$, $[Zn(PIC)_2(H_2O)_2] \cdot 2H_2O$, and $[Zn(HDIPIC)_2] \cdot 3H_2O$ were synthesized to correlate their thermal and spectral properties with crystal structures [26]. Surprisingly, zinc(II) pyridinecarboxylate biological activity was not detected until now.

To prepare silver(I) pyridinecarboxylates with perspective antimicrobial properties, we isolated AgPIC (**1**), AgNIC (**2**), and $[Ag(HDIPIC)] \cdot 0.75H_2O$ (**3**). Unfortunately, all attempts to obtain single crystals failed. Therefore, their compositions and molecular structures were described by indirect methods, elemental, spectral, and thermal analyses. The pyridinecarboxylate coordination was assigned by detailed mid-infrared spectral data and $\Delta(\nu_{as} - \nu_s)$ values; comparisons among free ligands and their Ag(I) complexes and sodium salts were accomplished. Moreover, we compared their spectral and thermal properties with Zn(II) analogs. $[Zn(PIC)_2(H_2O)_2] \cdot 2H_2O$ (**4**), $[Zn(NIC)_2(H_2O)_4]$ (**5**), and $[Zn(HDIPIC)_2] \cdot 3H_2O$ (**6**) were prepared in accord with our previous procedure [26]. The zinc(II) and silver(I) complexes' antimicrobial activities are discussed.

2. Experimental

2.1. *Materials and methods*

The pyridinecarboxylic acids (scheme 1), tetramethylammonium hydroxide pentahydrate ($(CH_3)_4N(OH) \cdot 5H_2O$) were obtained from Sigma-Aldrich and $AgNO_3$ from Lachema companies. All chemicals were analytically pure and used without purification.

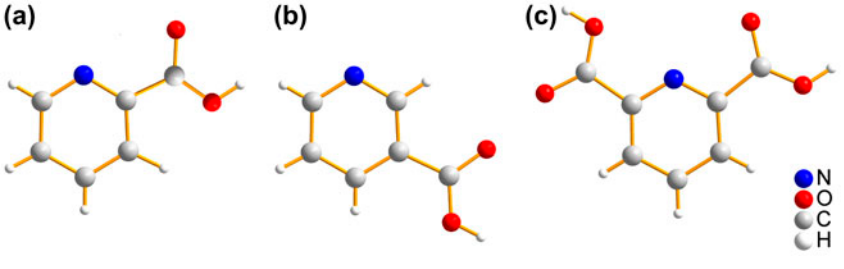

Scheme 1. The formulas of (a) picolinic acid, (b) nicotinic acid, and (c) dipicolinic acid.

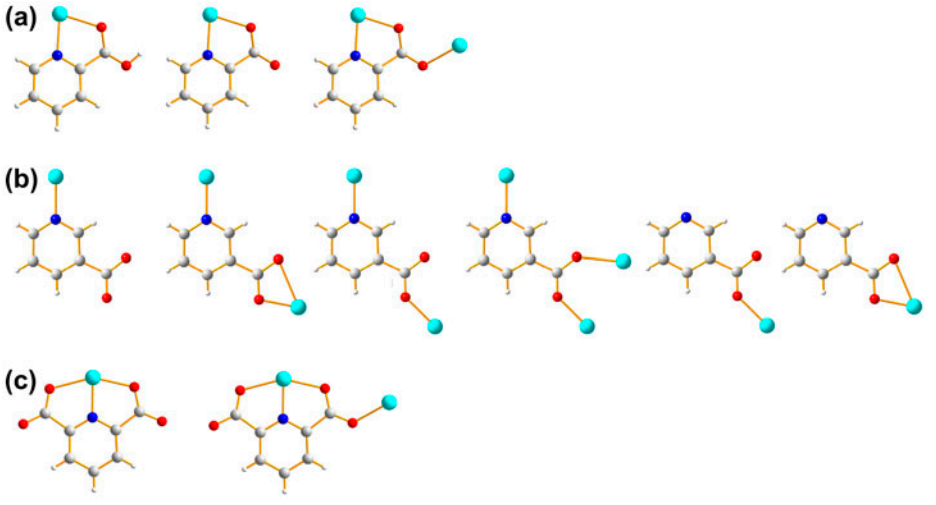

Scheme 2. Picolinate (a), nicotinate (b), and dipicolinate (c) coordination modes in CCDC.

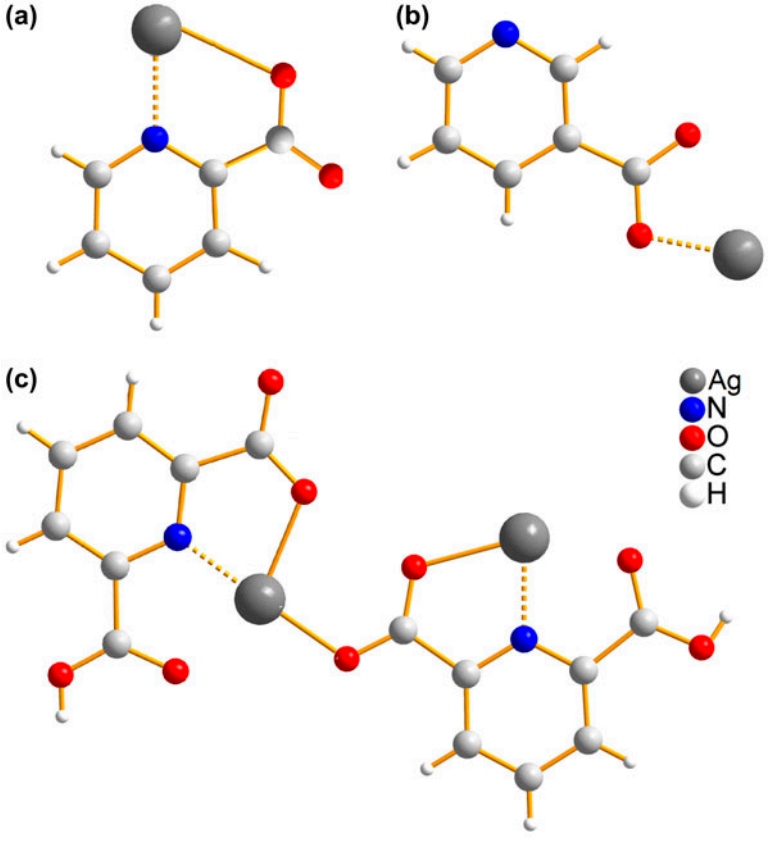

Scheme 3. The molecular diagram of **1**, **2**, and **3** derived from spectral studies. (a) AgPIC **(1)**, (b) AgNIC **(2)**, and (c) [Ag(HDIPIC)]·0.75H2O **(3)**.

Infrared spectra of the compounds were recorded on an Avatar FT-IR 6700 spectrometer from 4000 to 400 cm^{-1} using ATR (attenuated total reflectance) technique.

^1H NMR spectra were recorded in DMSO-d_6 with a Varian Mercury Plus 400 spectrometer at 400 MHz using TMS as the internal reference. Before NMR experiments, fresh samples of **1**, **2,** and **3** were dissolved for half an hour by ultrasonic homogenizer. After the ^1H NMR experiments, the samples were kept in the dark for 96 h and the measurements were repeated.

The elemental analysis was performed with CHNOS Elemental Analyzer vario MICRO from Elementar Analysensysteme GmbH. The TG/DTG and DTA measurements were carried out using TA instruments Netsch 409 PC. The mass of the samples was 15–20 mg. Samples were heated in air (50 $cm^3\,min^{-1}$) with heating rate 9 °C min^{-1} from 25 to 600 °C.

2.2. *Preparation of the Ag(I) complexes*

2.2.1. AgPIC (1) and AgNIC (2) complexes syntheses. Silver nitrate (139 mg $AgNO_3$, 0.818 mM) with picolinic acid (nicotinic acid) (100 mg $C_5H_4N(COOH)$, 0.812 mM) was strirred in DMF (10 mL). After dissolution, the reaction mixture was placed in a 40 mL Parr Teflon-lined stainless-steel vessel, which was heated to 90 °C with heating rate of 3 °C min^{-1} for 36 h. Then the reaction mixture was cooled to 70 °C with cooling rate of 0.1 °C min^{-1} and left at temperature for 12 h. Finally, the mixture was stepwise cooled to room temperature at 0.1 °C min^{-1}. Dry products were used for further characterization. Anal. Calcd for $AgC_6H_4NO_2$ (molar mass: 228.98 g M^{-1}) (98 mg, 52% yield (**1**)): C, 31.34%; H, 1.75%; N, 6.09%. Found: C, 31.02%; H, 1.83%; N, 6.03%. Anal. Calcd for $AgC_6H_4NO_2$ (molar mass: 228.98 g M^{-1}) (117 mg, 62% yield (**2**)): C, 31.34%; H, 1.75%; N, 6.09%. Found: C, 31.14%; H, 1.68%; N, 6.22%.

2.2.2. [Ag(HDIPIC)]·0.75H_2O (3) synthesis. Silver nitrate ((139 mg $AgNO_3$, 0.818 mM), dipicolinic acid (50 mg $C_5H_3N(COOH)_2$, 0.299 mM), and tetramethylammonium hydroxide pentahydrate (57 mg $N(CH_3)_4OH{\cdot}5H_2O$, 0.315 mM) were dissolved in 15 mL solvent mixture (volume ratio, ethanol : water, 1 : 1), placed in a 40 mL Parr Teflon-lined stainless-steel vessel, heated to 60 °C with heating rate of 3 °C min^{-1} for 36 h, and then slowly cooled at 1 °C min^{-1} to room temperature. White powder of **3** was separated by filtration, washed by ethanol, and dried. Anal. Calcd for $AgC_7H_{5.5}O_{4.75}N$ (molar mass: 287.49 g M^{-1}) (58 mg, 68% yield): C, 29.24%; H, 1.93%; N, 4.87%. Found: C, 29.05%; H, 1.90%; N, 4.85%.

2.3. *Antimicrobial activity*

The antibacterial activities of the Zn(II) and Ag(I) pyridinecarboxylate complexes and free ligands (picolinic, nicotinic, and dipicolinic acids (scheme 1)) were evaluated by micro-dilution using G^+ bacteria *Staphylococcus aureus* CCM 3953 and G^- bacteria *E. coli* CCM 3988 [27]. The effects of these compounds on the growth of yeasts *Candida parapsilosis* were determined by macro-dilution in L-shaped tubes adapted for direct measurement of absorbance [28]. Cultures of bacteria (in Mueller–Hinton growth medium) and yeasts (Sabouraud's growth medium) were incubated under vigorous shaking. The effects of the compounds on growth of filamentous fungi *Rhizopus oryzae* CCM F-8284, *Alternaria alternata* CCM F-128, and *Microsporum gypseum* CCM F-8342 were observed by macro-dilution on solidified broth medium during static culturing [29, 30] and the diameters of

growing fungal colonies were measured at intervals. Chromatographically pure compounds were dissolved in DMSO. Its final concentration never exceeded 1.0 vol. % in either control or treated samples. Concentration of the tested compounds was 0.1×10^{-3}–2.0 mM dm^{-3} in all experiments. The antimicrobial activity of the tested compound was characterized by IC_{50} values (concentration of a compound which in comparison to the control inhibits the growth of model microorganisms to 50%) and also by the minimal inhibitory concentration (MIC) values (MIC of a compound which inhibits microbial growth by 100%). The IC_{50} and MIC values were read from toxicity curves. MIC experiments on subculture dishes were used to assess the minimal microbicidal concentration (MMC). Subcultures were prepared separately in Petri dishes containing appropriate agar growth medium, and incubated at 30 °C for 48 h (bacteria, yeasts) and 25 °C for 96 h (filamentous fungi). The MMC value was taken as the lowest concentration which showed no visible growth of microbial colonies on the subculture dishes.

3. Results and discussion

Ag(I) pyridinecarboxylates were previously prepared by silver(I) salt and pyridinecarboxylate (or its acid) reaction at ambient temperature and atmospheric pressure in aqueous solution: silver(I) salts (nitrate, acetate, and fluoride) and nicotinic acid (molar ratio 1 : 2) from deionized water provided *catena*-H[Ag(NIC)$_2$] [18]; *catena*-{NH_4[Ag(NIC)$_2$]·H_2O} recrystallization from water containing sufficient ammonia provided *catena*-[Ag(NIC)] [19]. We used solvothermal conditions for new silver(I) pyridinecarboxylate preparation. Elemental, spectral, and thermal analyses (see below) confirm the formula of AgPIC (**1**), AgNIC (**2**), and [Ag(HDIPIC)]·0.75H_2O (**3**) from mixtures acquired at solvothermal conditions.

3.1. *IR spectral study*

Detailed analyses of IR spectra for **1**, **2,** and **3** were used to assign their coordination. In order to describe obvious changes, we compared IR spectra of free pyridinecarboxylates and their binary complexes. Significant absorptions are noted in table 1. More visual comparison is shown in figures 1–3. Moreover, ^{1}H NMR spectral data comparisons were carried out in order to indicate molecular structure and stability of **1**, **2,** and **3**. ^{1}H NMR spectra of free HPIC, HNIC, and H_2DIPIC and AgPIC (**1**), Ag(NIC) (**2**), and [Ag(HDIPIC)]·0.75H_2O (**3**) immediately after synthesis and after 96 h are plotted in figures 4–6. Assignment of the proton chemical shifts is shown directly in figures 4–6.

3.1.1. Free ligands. Free ligand IR spectra (figures 1–3) indicate that they associate by strong hydrogen bonds and therefore exist in monomeric (picolinic acid) and dimeric forms (nicotinic, dipicolinic acid). The significant ν(C=O) is shifted to lower values in the order picolinic (1708 cm^{-1}, intramolecular hydrogen bonding), nicotinic (1693 cm^{-1}, intermolecular hydrogen bonding), and dipicolinic acid (1689 cm^{-1}, intra- and intermolecular hydrogen bonding). Broad medium signals at 2700–1800 (HNIC), 2800–1900 (HPIC), and 2900–2000 (H_2DIPIC) cm^{-1} are caused by carboxylic O–H stretching vibrations connected to strong hydrogen bonds, similar as Käll [18] noted for nicotinic acid. In addition, the absorption bands with wavenumber ($\nu_{as}(COO^-)/\nu_s(COO^-)$ 1604/1450 (picolinic acid), 1592/1414 (nicotinic

Table 1. IR spectral data of free pyridinecarboxylic acids and their silver complexes (assignments, wavenumbers [cm^{-1}], and intensities).

Assignments	Wavenumbers [cm^{-1}] and intensities					
	HPIC	AgPIC	HNIC	AgNIC	H_2DIPIC	[Ag(HDIPIC)] ·0.75H_2O
v (OH)	–	3448(m, br)	–	3448(m, br)	–	3520(m)
v (CH)	3114(m)	3045(m), 2998(w)	3068(w)	3043(w), 3069(w), 3082(w)	3065(w)	3100(w), 3079(w)
v (C=O)	1708(m)	–	1693(s)	–	1689(s)	1718(m)
v_{as} (COO^-)	1604(m)	1611(s)	1592(m)	1594(s),	–	1563(s)
v (C=C)	1592(m), 1570(m), 1525(m)	1585(s), 1565(s), 1421(w)	1583(m)	1550(s)	1574(m), 1453(m)	1607(s), 1582(s)
v_s (COO^-)	1450(m)	1393(s)	1414(m)	1385(s)	1408(m)	1375(s)
v (C–O) + δ(OH)	1290(m)	–	1284(s)		1254(m)	1234(s)
δ (CCH)	1084(m), 960(m)	1167(w), 1087(w), 1045(m)	1172(m), 1102(m), 1072(m)	1196(w), 1115(w), 1089(w)	1155(m), 1084(m)	1182(m), 1158(m), 1085(m)
γ (CCH)	742(s), 672(s)	742(m), 698(m)	740(s)	759(m)	745(s)	757(s)
δ (COO^-)	702(s)	705(s)	688(s), 637(s)	705(m)	691(s), 645(s)	698(s)

Note: s – strong, m – medium, w – weak, br – broad.

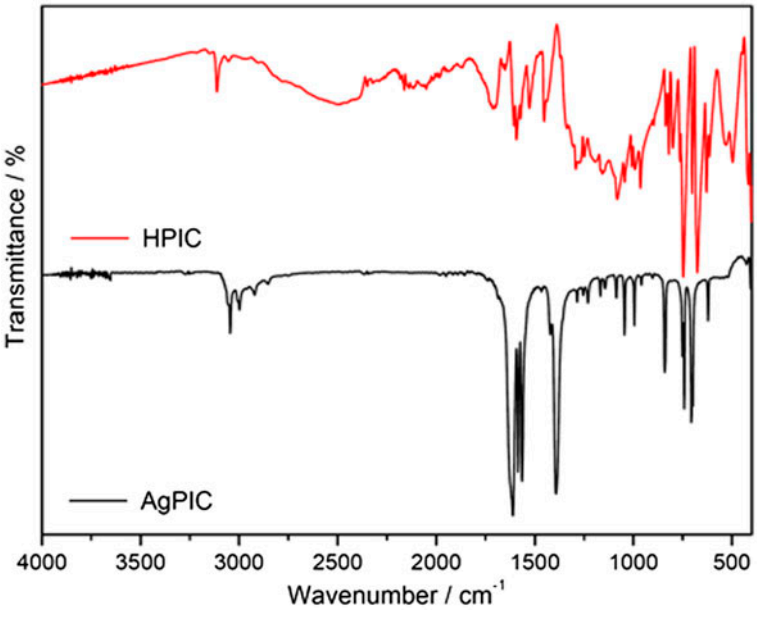

Figure 1. FT-IR spectra comparison of free HPIC and AgPIC.

acid), and 1574/1408 (dipicolinic acid) cm^{-1}) confirm the carboxylate asymmetric and symmetric vibrations. All further absorption bands are in agreement with published results [18].

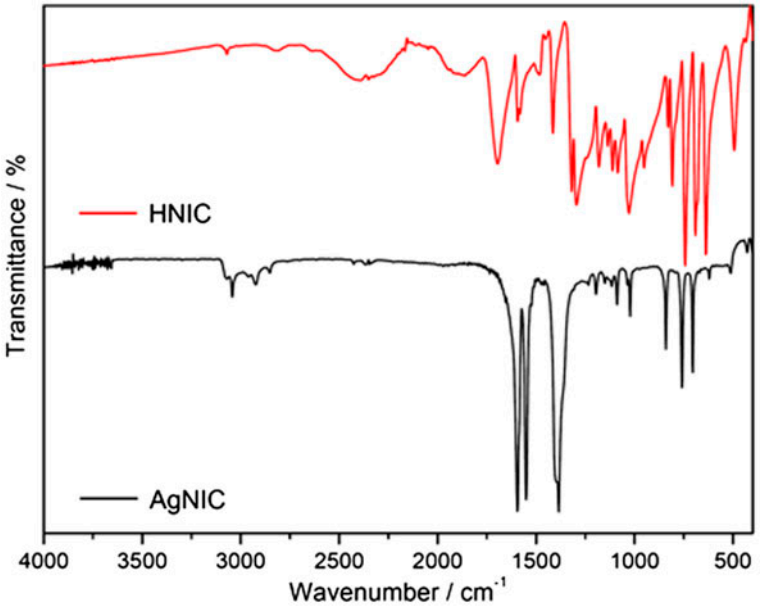

Figure 2. FT-IR spectra comparison of free HNIC and AgNIC.

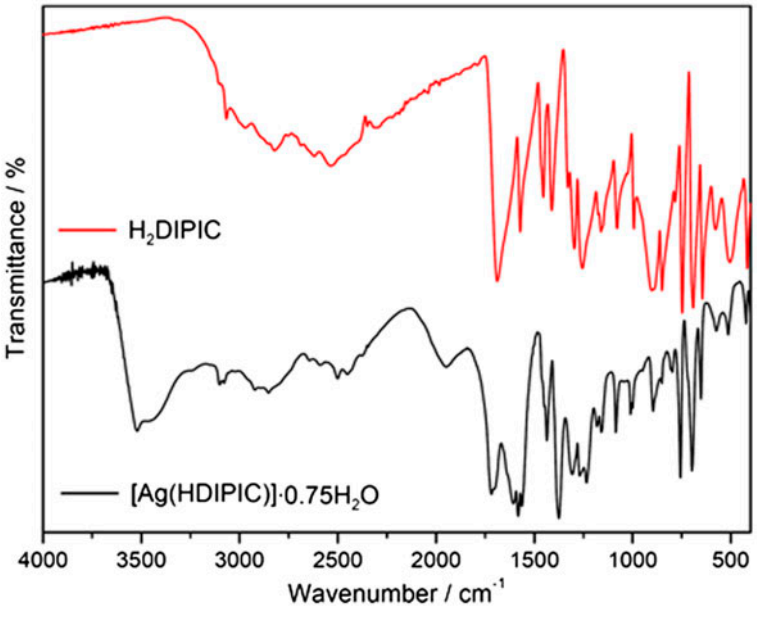

Figure 3. FT-IR spectra comparison of free H_2DIPIC and [Ag(HDIPIC)]·0.75H_2O.

^{1}H NMR spectra of free ligands (figures 4–6) confirm proton chemical shifts are in agreement with Spectral Database for Organic Compounds [31]. ^{1}H NMR spectra of silver(I) complexes indicate their stability for 96 h.

3.1.2. HPIC, AgPIC (1), HNIC, and AgNIC (2). The silver(I) picolinate and nicotinate IR spectra are similar. Therefore, common disscussion is offered. Comparing IR spectra of the picolinic (nicotinic) acid and their silver(I) complexes (figures 1 and 2; table 1), significant changes were observed, mainly under wavenumber 1750 cm^{-1} that indicate interactions between Ag(I) and pyridinecarboxylates. Very strong absorption at 1611 (1594) cm^{-1} was assigned to asymmetric stretch, $\nu_{as}(COO^-)$. Strong signals at 1585, 1565, and 1550 cm^{-1} belong to $\nu(C{=}C)_{ar}$. Carboxylate symmetric stretch $\nu_s(COO^-)$ are at 1393 (1385) cm^{-1}. Both deformation vibrations were observed, the *in-plane* bending modes δ(CCH) from 1200 to 1040 cm^{-1} and *out-of-plane* bending modes γ(CCH) from 740 to 690 cm^{-1}. Kalinowska *et al.* [21] presented similar wavenumbers, intensities, and assignments for picolinic acid and AgPIC complex.

To recognize PIC and NIC in silver(I) complexes from IR spectra, comparison was done from 1450 to 950 cm^{-1} [figure 7(a)]. The differences between 2- and 3-substituted pyridine derivatives can be identified by C–H *in-plane* bending vibrations of the pyridine ring. These vibrations are at 980–1300 cm^{-1}. The ring modes 1, 12, 18b, 9a, 15, 3 [figure 7(b)] and their absorption band positions in IR spectra are important makers which distinguish the picolinate and nicotinate molecules in their silver complexes. Park *et al.* [32] investigated adsorption of picolinic and nicotinic acids on silver sol surface at various pH values corresponding to cationic, zwitterion (N-protonated carboxylate structure), and anionic forms with simultaneous measurement of Raman spectra. Published results for anionic forms (NIC^-, PIC^-) were used for correlation of the silver(I) complexes in this study. The ring vibrations at 1022(1), 1036(12), 1150(9a), 1196(15), and 1234(3) cm^{-1} appeared in AgNIC spectra of our complex [figure 7(a) solid line]. Values correlate very well with reported values 1031(1), 1041(12), 1154(9a), 1196(15), and 1236(3) cm^{-1} for NIC^- [31]. The ring C–H vibrations at 995(1), 1045(12), 1085(18b), 1144(18b), 1254(15), and 1284(3) cm^{-1} for AgPIC [figure 7(a) dashed line] correlate with 1002(1), 1048(12), 1093(18b), 1150(18b), 1256 (15), and 1292(3) cm^{-1} values noted for PIC^- [31], respectively. However, ring mode 9a was not observed for PIC^- [32], but new ring mode 18b occurred. Based on the above comparison, the presence of picolinate and nicotinate molecules in silver complexes can be distinguished.

From Δ ($\Delta = (\nu_{as}(COO^-) - \nu_s(COO^-))$) [33, 34], the carboxylate coordination can be indicated. The Δ values 218 (209) cm^{-1} indicate monodentate carboxylate in AgPIC (AgNIC). To explain the observation, NaPIC (NaNIC) IR spectral data were also recorded (NaPIC: $\nu_{as}(COO^-) = 1606$, $\nu_s(COO^-) = 1412$, $\Delta = 194$ cm^{-1}; NaNIC: $\nu_{as}(COO^-) = 1613$, $\nu_s(COO^-) = 1408$, $\Delta = 205$ cm^{-1}). Comparing ours and published data ($\Delta = 217$ cm^{-1} for AgPIC, $\Delta = 223$ cm^{-1} for NaPIC [21], $\Delta = 196$ cm^{-1} for NaPIC, $\Delta = 206$ cm^{-1} for NaNIC [35]), ionic coordination of silver is preferred with particular monodentate carboxylate binding [scheme 3(a) and (b)], in agreement with thermal analysis (see below). Silver is chelated through pyridine nitrogen and oxygen carboxylate in AgPIC [scheme 3(a)] as the ^{1}H NMR study also indicates (figure 4, $\Delta\delta(H_d)$ is 0.11 ppm, $\Delta\delta(H_d) = \delta(H_d)$ free ligand – $\delta(H_d)$ complex, H_d is influenced by deprotonation of pyridine nitrogen and its coordination [36]). Similar 6-methylpicolinate (6-MePIC) coordination was observed in [Ag(6-MePIC)

(6-MeHPIC)] [37]. However, similar ethyl nicotinate (NICEt) provides N-pyridine coordination to silver(I) in [Ag(NICEt)]NO_3 [38].

Comparing Δ values with similar zinc(II) complexes (Δ {for $[Zn(NIC)_2(H_2O)_4]$} = 180 and {for $[Zn(PIC)_2(H_2O)_2]\cdot 2H_2O$} = 135 cm^{-1} [26], they are higher. These higher values indicate particular covalent character of carboxylate in silver(I) picolinate and nicotinate complexes, in agreement with Abarca's observation [22]. The chemical shift change of picolinic H_a (figure 4, $\Delta\delta(H_a)$ = 0.09 ppm) also confirms particular oxygen carboxylate interaction with silver. Similar differences were observed in picolinate connection to zinc [36]. Unfortunately, similar chemical shift differences were not observed in the silver(I)

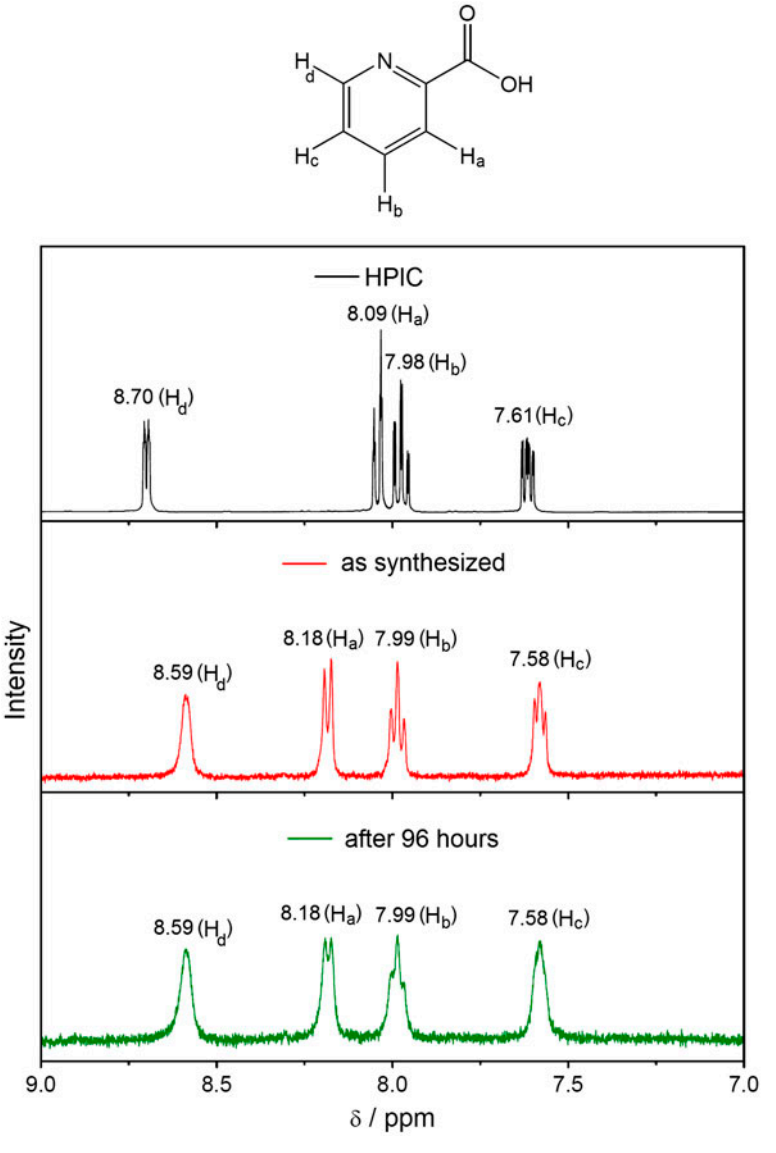

Figure 4. ^{1}H NMR spectra comparison of free HPIC and AgPIC.

nicotinate complex (figure 5) and zinc complexes [36]. The reduced Δ (from IR data) for $[Zn(NIC)_2(H_2O)_4]$ is explained by carboxylate hydrogen bonds [26]; the low Δ value for $[Zn(PIC)_2(H_2O)_2]\cdot 2H_2O$ is explained by chelate coordination through pyridine nitrogen and carboxylate oxygen and strong hydrogen network presence [26].

3.1.3. H_2DIPIC, [Ag(HDIPIC)]·0.75H_2O (3). Contrary to **1** and **2**, IR spectra for **3** (figure 3) are different. The medium broad signal (3000–2000 cm^{-1}) indicates the presence of the carboxylic O–H with strong hydrogen bonds. Simultaneously, the signal at 1718 cm^{-1} affirms the carbonyl presence in **3**. The *in-plane* bending modes δ(CCH) in wavenumber ranging from 1200 to 1040 cm^{-1} are more intense.

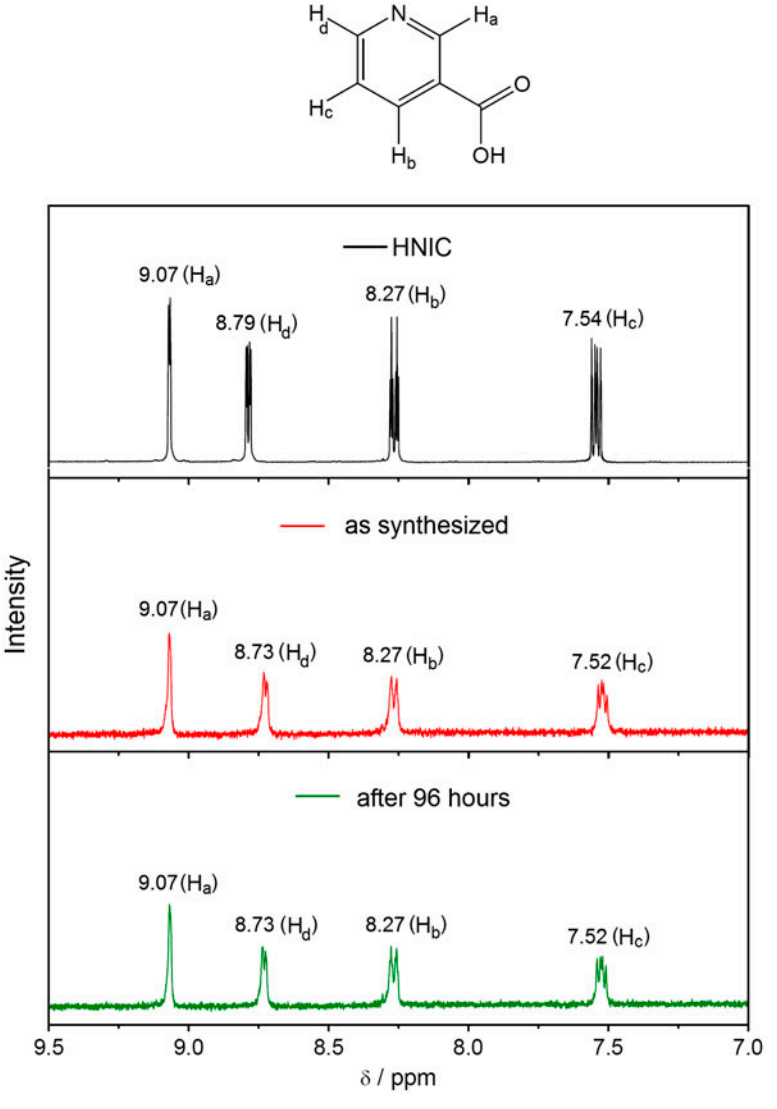

Figure 5. ^{1}H NMR spectra comparison of free HNIC and AgNIC.

Comparing the position of free ligand (figure 3; table 1) absorptions, significant changes were observed in free ligand and [Ag(HDIPIC)]·0.75H_2O spectra. The asymmetric and symmetric stretches at 1563 and 1375 cm^{-1}, respectively, confirm carboxylate coordination to silver(I). Comparison of ^1H NMR spectra (figure 6 of free dipicolinic acid and its silver (I) complex) indicates significant change in signals. These differences support silver(I) dipicolinate complex formation similar to zinc(II) dipicolinate [36]. The Δ comparison between sodium dipicolinate (Na_2DIPIC: $\nu_{as}(COO^-)$ = 1579, $\nu_s(COO^-)$ = 1387, Δ = 192 cm^{-1}) and **3** (Δ = 188 cm^{-1}) suggests combination of chelate and bridging coordination [scheme 3(c)].

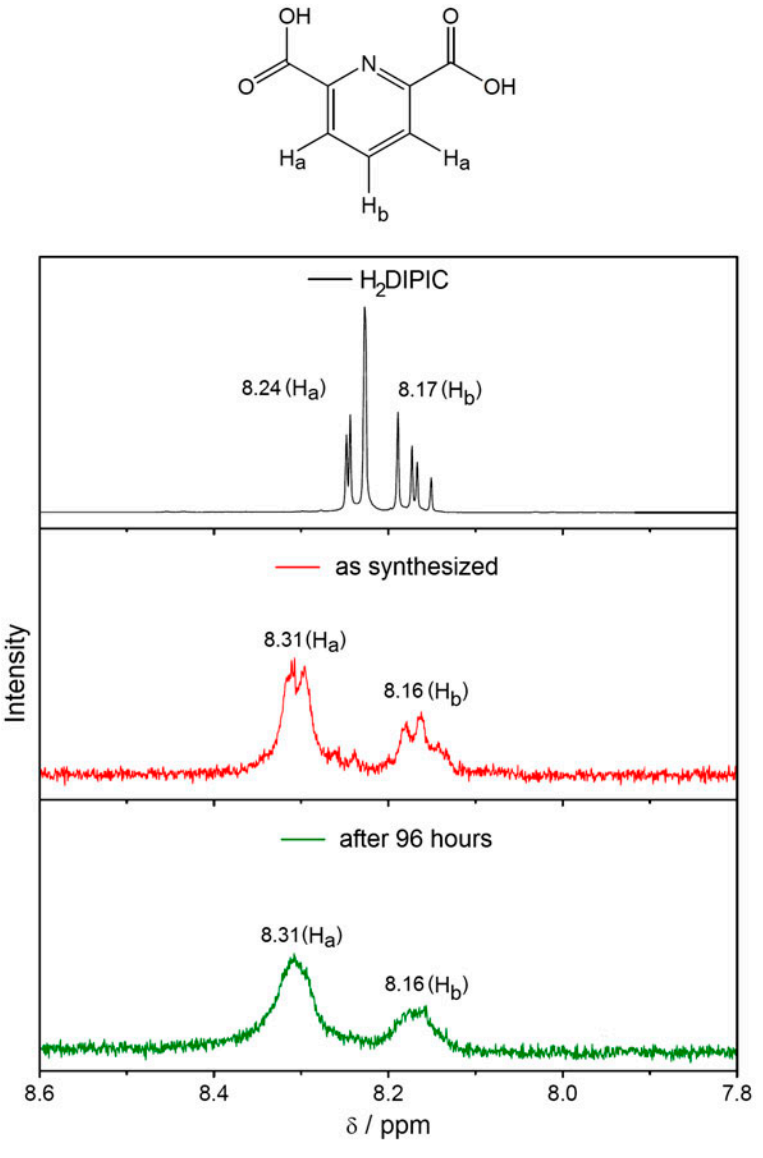

Figure 6. ^1H NMR spectra comparison of free H_2DIPIC and [Ag(HDIPIC)]·0.75H_2O.

Dimethyl dipicolinate (DIPICMe) and dipicolinate N-oxide (DIPICN-O) coordinate silver(I) by similar chelate coordination in *catena*-[Ag(DIPICMe)NO_3] [39] and *catena*-[Ag_2(DIPICN-O)] [40]. Distorted tetrahedral geometry around silver(I) is by two oxygens of nitrates (*catena*-[Ag(DIPICMe)NO_3]) and two kinds of Ag(I) exist in *catena*-[Ag_2(DIPICN-O)] [40].

Similar [$Zn(HDIPIC)_2$]·$3H_2O$ provides low Δ (140 cm^{-1}) in IR spectra [26]. Analogous to [$Zn(PIC)_2(H_2O)_2$]·$2H_2O$, chelate coordination (through pyridine nitrogen and carboxylate oxygen) and strong hydrogen bonds significantly influence Δ values [26].

3.2. *Thermal study*

AgPIC (**1**) thermoanalytical curves (TG/DTG-DTA) are shown in figure 8(a). Complex **1** is thermophylic up to 245 °C. The first mass loss is observed from 250 to 300 °C with both enthalpic effects, slightly endothermic (maximum at 250 °C) and slightly exothermic (maximum at 256 °C). This mass loss corresponds to pyridine release (34.7/34.0%, theor./obsd). Carbon dioxide is released in the following decomposition at 350–500 °C. An exothermic effect accompanies carbon dioxide release with maximum being at 440 °C. The experimental mass loss (19.1%) corresponds with calculated (18.1%). The solid residue after thermal decomposition is silver (47.4/46.9%, theor./obsd).

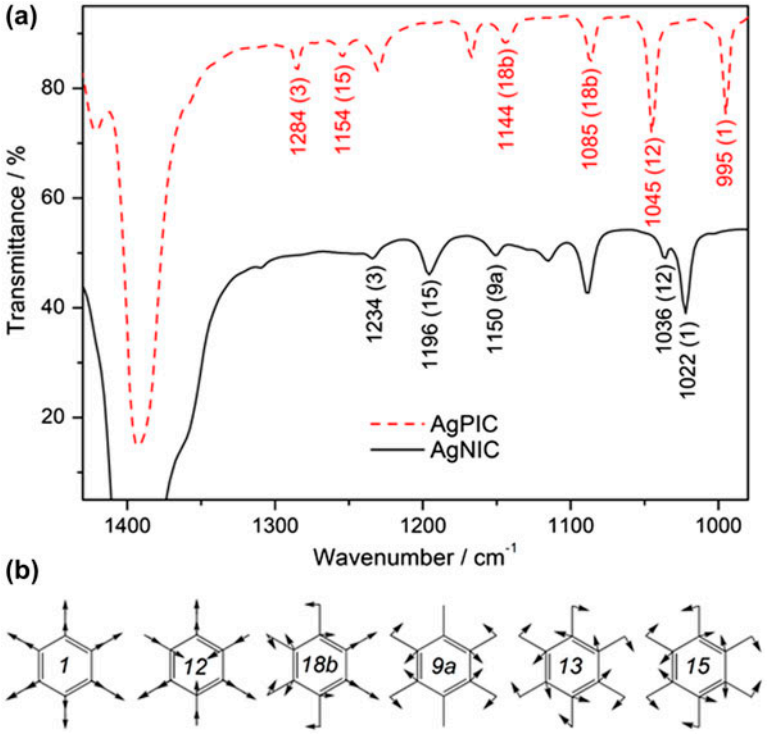

Figure 7. (a) FT-IR spectra of AgPIC (dashed line) and AgNIC (solid line) from 1450 to 950 cm^{-1}. (b) Scheme of C–H *in-plane* vibration ring modes 1, 12, 18b, 9a, 13 and 15.

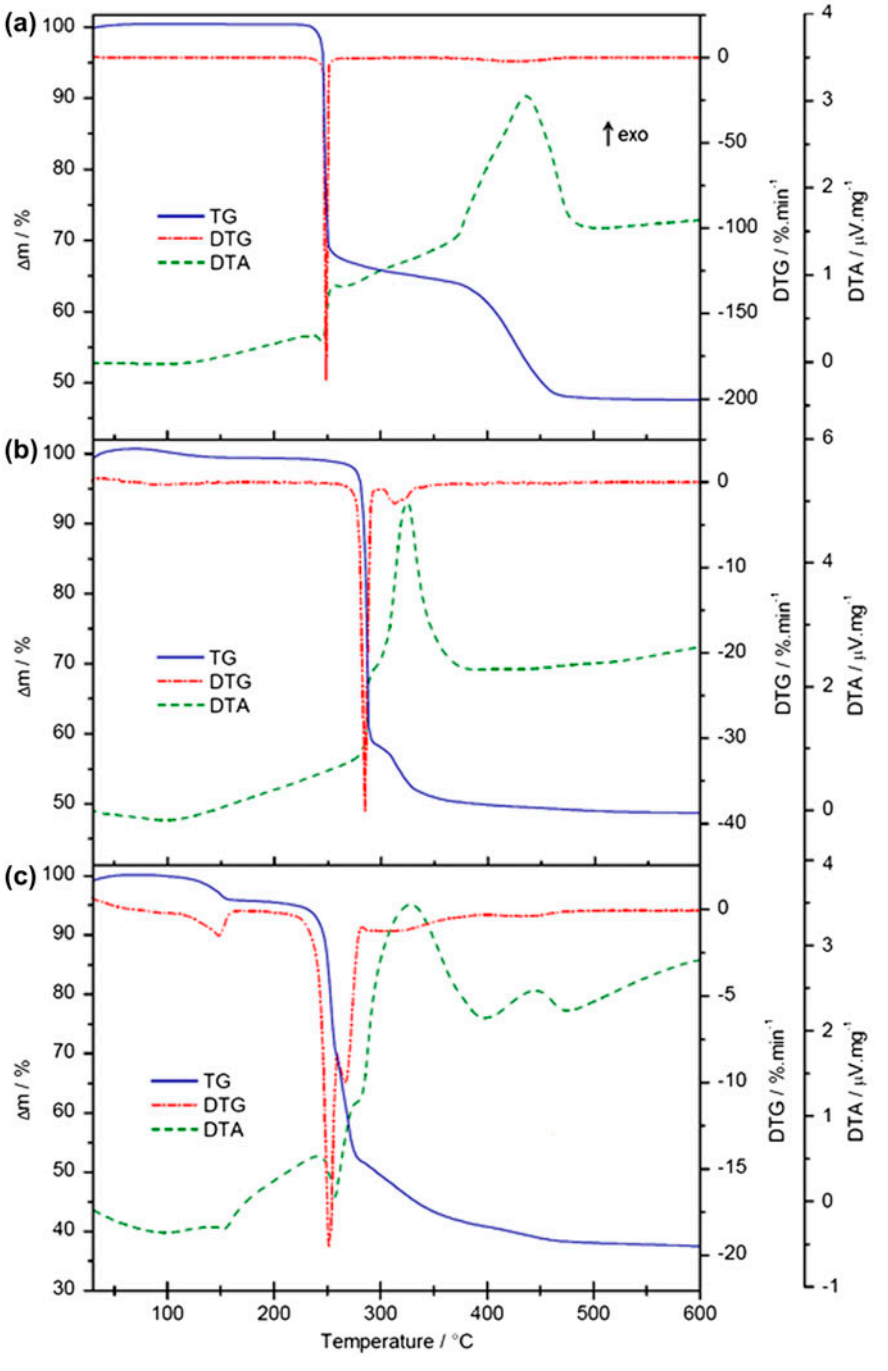

Figure 8. Thermoanalytical curves (TG/DTG-DTA) of (a) AgPIC, (b) AgNIC, and (c) [Ag(HDIPIC)]·0.75H_2O measured in air.

AgNIC (**2**) TG/DTG-DTA curves are shown in figure 8(b). Similar to **1**, **2** thermal decomposition is a one-step process. However, **2** is more thermophylic (270 °C) than **1** (245 °C). Nicotinate is released from the sample above this temperature. The experimental mass loss (51.0%) is in agreement with calculated (53.0%). The organic part of thermal pyrolysis is accompanied by an exothermic effect (250–400 °C, DTA curve maximum 330 °C) on the DTA curve. The solid residue is again silver (47.4/47.0%, theor./obsd).

[Ag(HDIPIC)]·0.75H_2O (**3**) TG/DTG-DTA curves are shown in figure 8(c). The hydrated **3** is the least thermophylic (110 °C). A complex dehydration occurs from 110 to 160 °C with DTA curve maximum at 153 °C and 0.75 water molecules released (mass loss 4.7/4.5%, theor./obsd). The organic pyrolysis at 220–520 °C is slightly endothermic (DTA curve maximum at 260 °C) and more significantly exothermic (DTA curve maximum 330, 440 °C). The mass loss indicates dipicolinate release (57.8/57.8%, theor./obsd). Similar to previous cases, the solid residue is metal silver (37.5/38.4%, theor./obsd).

We compared the anhydrous zinc(II) and silver(I) pyridinecarboxylates' thermal stability, and the order is similar:

$$\mathrm{Ag(HDIPIC)}(225\,^{\circ}\mathrm{C}) < \mathrm{Ag(PIC)}(245\,^{\circ}\mathrm{C}) < \mathrm{Ag(NIC)}(270\,^{\circ}\mathrm{C})$$

$$\mathrm{Zn(HDIPIC)_2}(200\,^{\circ}\mathrm{C}) < \mathrm{Zn(PIC)_2}(300\,^{\circ}\mathrm{C}) < \mathrm{Zn(NIC)_2}(390\,\circ\mathrm{C})$$

Zinc(II) complexes are more stable than silver(I) from carboxylate oxygen connection to zinc(II) forming polymeric (in the $Zn(NIC)_2$) and chelate picolinate coordination to zinc(II) (in the $Zn(PIC)_2$) [26]. The lowest thermal stabilities of $Zn(HDIPIC)_2$ and Ag(HDIPIC) are caused by C–C bonds splitting in the hydrogenpicolinate anion [26]. The prevalent ionic coordination mode in anhydrous silver(I) picolinate and nicotinate complexes causes their lower thermal stability than in similar zinc(II) complexes.

3.3. *Antimicrobial activity*

3.3.1. Zn complexes. Antimicrobial activity of free ligands and their Zn^{2+} complexes (figure 9) characterized by IC_{50} and MIC values is summarized in table 2.

HPIC, HNIC, and H_2DIPIC were antimicrobially inactive against bacteria G^+ *S. aureus*, G^- *E. coli*, yeasts *C. parapsilosis*, and filamentous fungi *R. oryzae*, *A. alternata*, *M. gypseum*. Their IC_{50} and MIC values are higher than 2 mM dm^{-3}, except H_2DIPIC against yeasts *C. parapsilosis* – $IC_{50} = 1.1$ and MIC–2 mM dm^{-3}.

The presence of zinc(II) in picolinate and nicotinate complexes led to increase of antibacterial activity. Comparing IC_{50} and MIC values, the zinc(II) nicotinate complex has the highest antibacterial activity towards both bacteria: $IC_{50} = 0.2$ (*S. aureus*), 0.5 (*E. coli*) mM dm^{-3}, and MIC = 2 mM dm^{-3}, with bacteriostatical effect on bacterial cells.

Similar to bacteria, zinc(II) nicotinate complex affords the highest activity against pathogenic yeasts *C. parapsilosis* – $IC_{50} = 0.23$ and MIC = 0.5 mM dm^{-3} with fungistatic effect on yeasts cells.

Zinc(II) nicotinate (*A. alternata* – $IC_{50} = 1.3$ and MIC > 2 mM dm^{-3}) ligands nor their zinc(II) complexes do not repress growth of filamentous fungi *R. oryzae*, *A. alternata*, *M. gypseum* (IC_{50} and MIC > 2 mM dm^{-3}). Comparing IC_{50} and MIC values, inhibition activity of the Zn(II) complexes decreases in the order: $[Zn(NIC)_2(H_2O)_4]$ > $[Zn(PIC)_2(H_2O)_2]\cdot 2H_2O$ > $[Zn(HDIPIC)_2]\cdot 3H_2O$. Comparing Zn(II) picolinate ($[(Zn(PIC)_2(H_2O)_2]\cdot 2H_2O$) and

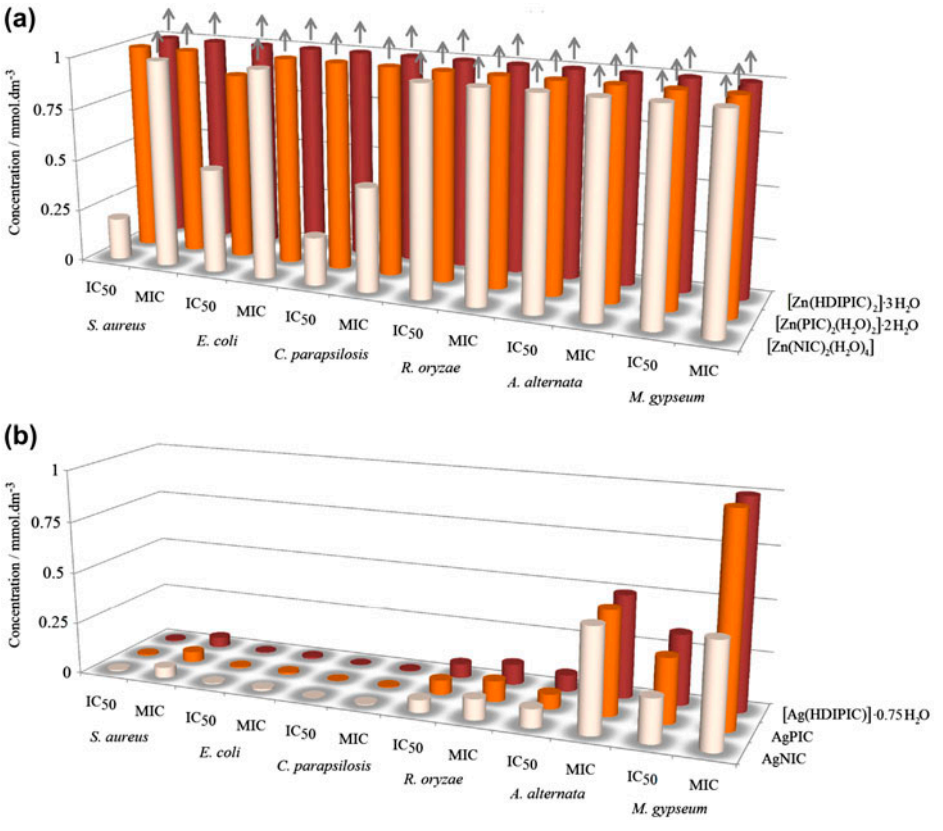

Figure 9. Antimicrobial activity of zinc(II) and silver(I) complexes characterized by IC_{50} and MIC values.

salicylate ($[Zn(SALIC)_2]\cdot 2H_2O$) antimicrobial activity, Zn(II) picolinate affords comparable activity like Zn(II) salicylate [41].

3.3.2. Ag complexes. The IC_{50} and MIC values are noted in table 2 for free ligands and their Ag(I) complexes (figure 9).

Growth of *S. aureus* and *E. coli* is significantly suppressed by silver(I) complexes present in growth medium (see table 2); 50% growth inhibition of both bacteria by AgPIC, AgNIC, and $[Ag(HDIPIC)]\cdot 0.75H_2O$ is similar, with IC_{50} ranging from 0.005 to 0.007 mM dm^{-3}. Total (100%) growth inhibition of *S. aureus* was observed at 0.05 mM dm^{-3} for all silver(I) complexes but with bactericide effect for AgPIC and AgNIC and bacteristatic effect for $[Ag(HDIPIC)]\cdot 0.75H_2O$. Hundred percent growth inhibition of *E. coli* was observed for all silver(I) complexes (even at five times lower concentration of 0.01 mM dm^{-3}) with bacteristatic effect.

Silver(I) complexes significantly influence the growth of *C. parapsilosis* yeast (see table 2). Similar to bacteria, anti-yeast activity of AgPIC, AgNIC, and $[Ag(HDIPIC)]\cdot 0.75H_2O$ is approximately the same, IC_{50} of 0.9–1.0 μM dm^{-3}. The total growth inhibition (MIC = 0.005 mM dm^{-3}) with fungistatic effect toward the yeast cells was noted. Comparing IC_{50} and MIC values, anti-yeast activity is higher than antibacterial. Similar to previous cases, silver presence increases antifungal activity.

Table 2. Antimicrobial activity of free pyridinecarboxylic ligands and their zinc(II) and silver(I) complexes.

	Bacteria				Yeasts				Filamentous fungi			
	S. aureus		*E. coli*		*C. parapsilosis*		*R. oryzae*		*A. alternata*		*M. gypseum*	
	IC_{50}	MIC	IC_{50}	MIC	IC_{50}	MIC	IC_{50}	MIC	IC_{50}	MIC	IC_{50}	MIC
$[Zn(PIC)_2(H_2O)_2]\cdot 2H_2O$	1	>2	0.9	>2	>2	>2	>2	>2	>2	>2	>2	>2
$[Zn(NIC)_2(H_2O)_4]$	0.2	2s	0.5	2s	0.23	0.5s	>2	>2	1.3	>2	>2	>2
$[Zn(HDIPIC)_2]\cdot 3H_2O$	>2	>2	>2	>2	>2	>2	>2	>2	>2	>2	>2	>2
AgPIC	0.007	0.05s	0.006	0.01s	0.001	0.005s	0.07	0.1c	0.07	0.5s	0.31	1s
AgNIC	0.006	0.05c	0.006	0.01s	0.001	0.005s	0.06	0.1c	0.09	0.5s	0.21	0.5s
$[Ag(HDPIC)]\cdot 0.75H_2O$	0.007	0.05c	0.005	0.01s	0.0009	0.005s	0.07	0.1c	0.08	0.5s	0.34	1s
HPIC	>2	>2	>2	>2	>2	>2	>2	>2	>2	>2	>2	>2
HNIC	>2	>2	>2	>2	>2	>2	>2	>2	>2	>2	>2	>2
H_2DIPIC	>2	>2	>2	>2	1.1	>2	>2	>2	>2	>2	>2	>2

Note: s – microbistatical effect, c – microbicidal effect.

Fungi growth inhibition decreased in the order: *R. oryzae* > *A. alternata* > *M. gypseum*. Antifungal activity of AgPIC, AgNIC, and [Ag(HDIPIC)]·0.75H_2O is approximately the same with IC_{50} of 0.06–0.07, MIC = 0.1 mM dm^{-3} (*R. oryzae*); IC_{50} of 0.07–0.09, MIC = 0.5 mM dm^{-3} (*A. alternata*) and IC_{50} of 0.21–0.34, MIC = 0.5–1.0 mM dm^{-3} (*M. gypseus*). Hundred percent growth inhibition with lethal effect on *R. oryzae* spores was observed at 0.1 mM dm^{-3} complex concentration. Total growth inhibition of *A. alternata* by all Ag(I) complexes with fungistatic effect on spores was recorded at 0.5 mM dm^{-3}. The highest growth inhibition of dermatophytic *M. gypseus* was observed by AgNIC.

By comparing IC_{50} and MIC values, we conclude that Ag(I) complexes inhibition activity against filamentous fungi decreases AgNIC > AgPIC > [Ag(HDIPIC)]·0.75H_2O.

Rowan *et al.* [42] with similar inactive N or O-donors (imidazole, salicylic acid, 2-methyl-5-nitroimidazole, 1-(3-aminopropyl)imidazole) tested against the pathogenic bacteria *S. aureus*, *E. coli*, and fungal pathogen *C. albicans*. Their MIC values are higher than 0.05 mM dm^{-3}. Their silver(I) complexes exhibited significantly greater antifungal (MIC_{100} values from 0.1 to 4.8 μM dm^{-3}) than antibacterial activity (MIC_{50} values from 0.0105 to 0.05 mM dm^{-3}). Similar trend is observed for our silver(I) complexes (MIC = 0.005 mM dm^{-3} for fungal pathogen *C. parapsilosis*, 0.01 and 0.05 mM dm^{-3} for pathogenic bacteria *E. coli* and *S. aureus*, respectively, see table 2).

Silver(I) complexes with 2-aminopyridine and 3-aminopyridine were tested against the Gram positive and negative bacteria and fungal pathogen [43]. Our silver(I) pyridinecarboxylate analogs (AgPIC (**1**) and AgNIC (**2**)) are more active against *E. coli* (MIC = 0.01 mM dm^{-3}) and *S. aureus* (MIC = 0.05 mM dm^{-3}) than their amino analogs (MIC = 0.054 mM dm^{-3} (*E. coli*)/0.433 mM dm^{-3} (*S. aureus*)), complex with 2-aminopyridine; MIC = 0.03 mM dm^{-3} (*E. coli*)/0.121 mM dm^{-3} (*S. aureus*), complex with 3-aminopyridine) [36].

Abarca *et al.* [22] tested AgNIC (composition stoichiometry $Ag(NIC)_2$) and AgPIC ($Ag(PIC)_2·H_2O$) against *E. coli* and *S. agalactiae* bacteria. Similarly, their complexes show lower antibacterial activity (IC_{50} = 0.044 mM dm^{-3} *E. coli*, IC_{50} = 0.067 mM dm^{-3} *S. agalactiae*, AgPIC; IC_{50} = 0.042 mM dm^{-3} *E. coli*, IC_{50} = 0.042 mM dm^{-3}, *S. agalactiae*, AgNIC) than our complexes (table 2). The differences are probably caused by lower silver (I) ion composition (29.1% Ag in $Ag(PIC)_2·H_2O$, 30.5% Ag in $Ag(NIC)_2$ [22], 46.7% Ag in AgPIC/AgNIC).

The Ag(I) pyridinecarboxylate antimicrobial activities (IC_{50} and MIC values) (figure 9) comparison leads to the following order: AgNIC > AgPIC > [Ag(HDIPIC)]·0.75H_2O, in agreement with increasing antimicrobial activity of silver(I) complexes influenced by ligand [22]. The AgPIC and AgNIC complexes, predominantly with ionic interaction, provide the most efficient antimicrobial effect (alternatively, the ligand exchange reaction, between pyridinecarboxylate and biological ligand, is easy), similar to Abarca's conclusion [22]. On the other hand, [Ag(HDIPIC)]·0.75H_2O (with chelate and bridging coordination mode, see above section 3.1.3) has the lowest antimicrobial effect.

Comparing Zn(II) and Ag(I) pyridinecarboxylate antimicrobial properties, the tested Zn (II) pyridinecarboxylates have lower antimicrobial effect than analogous silver(I) pyridinecarboxylates. However, the inhibition activity order is similar:

$$[Zn(NIC)_2(H_2O)_4] > [Zn(PIC)_2(H_2O)] \cdot 2H_2O > [Zn(HDIPIC)_2] \cdot 3H_2O$$

Their decreased antimicrobial activity is probably caused by more stable complexes, lower antimicrobial metal composition, or different ligand coordination.

4. Summary

Three silver(I) pyridinecarboxylates (AgPIC (**1**), AgNIC (**2**), [Ag(HDIPIC)]·0,75H_2O (**3**)) were prepared. Spectral, elemental, and thermal analyses were used for composition confirmation. Moreover, IR spectra data analysis provides the coordination mode. It confirms prevalent ionic interaction between silver(I) and picolinate and nicotinate with particular covalent character of interaction in the case of **2** and chelate character in **1**. The combination of chelate (through pyridine nitrogen and carboxylate oxygen) and bridging coordination mode (between the two central atoms) in hydrated **3** was observed. Pyridinecarboxylate coordination was compared to other silver(I) pyridinecarboxylate analogs (methyl and ethyl derivatives). Similar chelate coordination behavior was observed for picolinate and dipicolinate and different N-pyridine coordination in nicotinate. Thermal and structural property correlation among zinc(II) and silver(I) complexes were offered. The anhydrous zinc(II) pyridinecarboxylates form more stable complexes than silver(I). The silver(I) pyridinecarboxylates have significantly higher growth inhibition of model bacteria, yeasts, and filamentous fungi. Binding modes, antimicrobial metal, and complex stability can influence their antimicrobial activity.

Acknowledgements

Financial support was provided by grants of the Ministry of the Education of the Slovak Republic (VEGA 1/0366/14). The authors are very grateful to Miroslav Psotka, Mária Vilková, and Ján Imrich from P.J. Šafárik University in Košice for the NMR spectra measurement.

References

[1] G.D. Wright. *Curr. Opin. Microbiol.*, **13**, 589 (2010).
[2] U. Schatzschneider, N. Metzler-Nolte. *Angew. Chem. Int. Ed.*, **45**, 1504 (2006).
[3] J. Lv, T. Liu, S. Cai, X. Wang, L. Liu, Y. Wang. *J. Inorg. Biochem.*, **100**, 1888 (2006).
[4] G. Jaouen, P.J. Dyson. In *Comprehensive Organometallic Chemistry III, Medicinal Organometallic Chemistry*, D. O'Hare (Ed.), pp. 445–464, Elsevier, Amsterdam (2007).
[5] I. Bertini, H.G. Gray, E.I. Stiefel, J.S. Valentine. *Biological Inorganic Chemistry (Structure and Reactivity)*, University Science Books, Sausalito, CA (2007).
[6] S. Sayen, A. Carlier, M. Tarpin, E. Guillon. *J. Inorg. Biochem.*, **120**, 39 (2013).
[7] H.A. Krebs, D. Wiggins, M. Stubbs, A. Sols, F. Bedoya. *Biochem. J.*, **214**, 657 (1983).
[8] P.A. Mackowiak. *Clin. Infect. Dis.*, **31**, 154 (2000).
[9] P.J. Aggett, P.K. Fenwick, H. Kirk. *J. Nutr.*, **119**, 1432 (1989).
[10] C. Dazzi, G. Candiano, S. Massazza, A. Ponzetto, L. Varesio. *J. Chromatogr. B*, **751**, 61 (2001).
[11] T. Brody. *Nutritional Biochemistry*, 2nd Edn, Academic Press, San Diego, CA (1999).
[12] D. Cervantes-Laurean, N.G. McElvaney, J. Moss. In *Modern Nutrition in Health and Disease*, M. Shils, J.A. Olson, M. Shike, A.C. Ross (Eds), 9th Edn, pp. 442–451, Williams & Wilkins, Baltimore, MD (1999).
[13] R. Jacob, M. Swenseid. In *Present Knowledge in Nutrition*, E.E. Ziegler, L.J. Filer (Eds), 7th Edn, pp. 185–190, ILSI Press, Washington, DC (1996).
[14] M.K. Jacobson, E.L. Jacobson. *Trends Biochem. Sci.*, **24**, 415 (1999).
[15] T.A. Sliemandagger, W.L. Nicholson. *Appl. Environ. Microbiol.*, **67**, 1274 (2001).
[16] M.L. Cable, J.P. Kirby, K. Sorasaenee, H.B. Gray, A. Ponce. *J. Am. Chem. Soc.*, **129**, 1474 (2007).
[17] J.P. Deloume, R. Faure, H. Loiseleur. *Acta Crystallogr., Sect. B*, **33**, 2709 (1977).
[18] P.O. Käll, J. Grins, M. Fahlman, F. Söderlind. *Polyhedron*, **20**, 2747 (2001).
[19] G. Smith, A.N. Reddy, K.A. Byriel, C.H.L. Kennard. *Polyhedron*, **13**, 2425 (1994).
[20] M.G.B. Drew, R.W. Matthews, R.A. Walton. *J. Chem. Soc. A*, 1405 (1970).
[21] M. Kalinowska, M. Borawska, R. Świsłocka, J. Piekut, W. Lewandowski. *J. Mol. Struct.*, **834–836**, 419 (2007).

[22] R. Abarca, G. Gomez, C. Velasquez, M.A. Paez, M. Gulppi, A. Arrieta, M.I. Azocar. *Chin. J. Chem.*, **30**, 1631 (2012).
[23] C.L. Fox, S.M. Modak. *Antimicrob. Agents Chemother.*, **5**, 582 (1974).
[24] Z. Guo, P.J. Sadler. *Angew. Chem. Int. Ed.*, **38**, 1512 (1999).
[25] S. Ahmad, A.A. Isab, S. Ali, A.R. Al-Arfaj. *Polyhedron*, **25**, 1633 (2006).
[26] Z. Vargová, V. Zeleòák, I. Císaøová, K. Györyová. *Thermochim. Acta*, **423**, 149 (2004).
[27] S. Jantová, D. Hudecová, Š. Stankovský, K. Špirková, Ľ. Ružeková. *Folia Microbiol.*, **40**, 611 (1995).
[28] V. Betina, D. Mičeková. *Z. Allg. Mikrobiol.*, **5**, 55 (1972).
[29] D. Hudecová, S. Jantová, M. Melník, M. Uher. *Folia Microbiol.*, **40**, 473 (1996).
[30] B. Dudová, D. Hudecová, R. Pokorný, M. Mičková, M. Palicová, P. Segl'a, M. Melník. *Folia Microbiol.*, **47**, 225 (2002).
[31] Free access http://sdbs.riodb.aist.go.jp/sdbs/cgi-bin/direct_frame_top.cgi.
[32] S.M. Park, K. Kim, M.S. Kim. *J. Mol. Struct.*, **344**, 195 (1995).
[33] G.B. Deacon, R.J. Phillips. *Coord. Chem. Rev.*, **33**, 227 (1980).
[34] Z. Vargová, M. Almáši, L. Arabuli, K. Györyová, V. Zeleňák, J. Kuchár. *Spectrochim. Acta Part A*, **78**, 788 (2011).
[35] A. Szorcsik, L. Nagy, J. Sletten, G. Szalontai, E. Kamu, T. Fiore, L. Pellerito, E. Kálmán. *J. Organomet. Chem.*, **689**, 1145 (2004).
[36] Z. Vargová, J. Kotek, J. Rudovský, J. Plutnar, R. Gyepes, P. Hermann, K. Györyová, I. Lukeš. *Eur. J. Inorg. Chem.*, **25**, 3974 (2007).
[37] A. Leiva, W. Clegg, L. Cucurull-Sánchez, P. González-Duarte, J. Pons. *J. Chem. Crystallogr.*, **29**, 1097 (1999).
[38] M.A.M. Abu-Youssef, R. Dey, Y. Gohar, A.A. Massoud, L. Öhrström, V. Langer. *Inorg. Chem.*, **46**, 5893 (2007).
[39] M. Hakimi, K. Moeini, Z. Mardani, E. Schuh, F. Mohr. *J. Coord. Chem.*, **66**, 1129 (2013).
[40] W.P. Wu, Y.Y. Wang, C.J. Wang, Y.P. Wu, P. Liu, Q.Z. Shi. *Inorg. Chem. Commun.*, **9**, 645 (2006).
[41] Z. Bujdošová, K. Gyoryová, J. Kovarová, D. Hudecová, L. Halás. *J. Therm. Anal. Calorim.*, **98**, 151 (2009).
[42] R. Rowan, T. Tallon, A.M. Sheahan, R. Curran, M. McCann, K. Kavanagh, M. Devereux, V. McKee. *Polyhedron*, **25**, 1771 (2006).
[43] M.A.M. Abu-Youssef, V. Langer, L. Ohrström. *Dalton Trans.*, 2542 (2006).